

Motions of Tetramethylammonium Cations and Phase Transitions in Solid $[(\text{CH}_3)_4\text{N}]_2\text{CdX}_4$ ($\text{X}=\text{Cl}, \text{Br}, \text{I}$) as Studied by ^1H NMR, Powder X-Ray Diffraction, and Differential Thermal Analysis Measurements

Setsuko SATO, Ryuichi IKEDA, and Daiyu NAKAMURA*

Department of Chemistry, Faculty of Science, Nagoya University, Chikusa-ku, Nagoya 464

(Received January 31, 1986)

The temperature dependences of ^1H spin-lattice relaxation times were determined at 20 MHz for $[(\text{CH}_3)_4\text{N}]_2\text{CdCl}_4$, $[(\text{CH}_3)_4\text{N}]_2\text{CdBr}_4$, and $[(\text{CH}_3)_4\text{N}]_2\text{CdI}_4$. For the last two complexes, the frequency dependence of the relaxation time was observed above room temperature. ^1H NMR second moments were observed for the bromide complex. At room temperature, the first two complexes were found to be isomorphous with the iodide complex which forms orthorhombic crystals. Differential thermal analysis experiments revealed that these complexes undergo four, one, and one solid-solid phase transitions in the above order between ca. 80 and 430 K. Two ^1H T_1 minima were clearly observed at lower temperatures for the chloride and bromide complexes, whereas at least three ^1H T_1 minima partly overlapped with each other were detected at lower temperatures for the iodide complex. For the former two complexes, the ^1H T_1 data were well analyzed by the general method already reported. For the bromide and iodide complexes, ^1H T_1 curves observed showed a maximum above room temperature. Motions of the cation activated in these complexes are discussed in relation to the crystal field experienced by the cation.

Dynamic behavior of tetramethylammonium (tetMA)⁺ cations in various crystalline salts has been studied fairly in detail by means of ^1H NMR techniques.¹⁻¹²⁾ The motions of the cation contributing to ^1H spin-lattice relaxation times (T_1) around room temperature have been shown to be random reorientations of CH_3 groups about each C-N bond axis by 120° , i.e., the C_3 reorientations, and overall reorientations of the cations about the center of gravity. It has been revealed through the temperature dependence measurements of ^1H T_1 that the activation energies (E_a) for the CH_3 C_3 reorientation of the above salts except (tetMA) CdCl_3 ¹²⁾ are in a range of 15–30 kJ mol⁻¹. The widely spread values of E_a observed indicate that the potential barriers to reorient arising from interionic as well as intraionic forces contribute to E_a for the CH_3 C_3 reorientation of the cation.

When the cations are located in a weak crystal field formed by surroundings such as those in (tetMA)₂MBr₆ (M=Sn, Te, Pt), E_a for the CH_3 C_3 reorientation is thought to be mostly determined by the intraionic potential barrier.¹⁰⁾ In these crystals, the four CH_3 groups in the cation are equivalent because of the position of the cation having a high site symmetry and the E_a values observed are ca. 17 kJ mol⁻¹. If the cation is placed at a low-symmetric lattice site, however, it is supposed that the cation is somewhat distorted owing to an asymmetric crystal field and the four CH_3 groups become nonequivalent. For the distorted cations, we can expect that they show ^1H T_1 through unique motional processes different from those found for the high symmetric cations. In the present investigation, we have selected (tetMA)₂CdX₄ (X=Cl, Br, I) as an example of the salts having the cations distorted and the measurements of the temperature dependences of ^1H NMR parameters, X-ray powder diffraction, and differential thermal analysis (DTA)

have been undertaken to obtain detailed information about the motion of the slightly distorted cations.

Experimental

Wide-line ^1H NMR absorptions were recorded to evaluate ^1H NMR second moments (M_2) at several temperatures by use of a JEOL JNM-MW-40S spectrometer operated at 40 MHz. The temperature dependences of ^1H T_1 were measured at the Larmor frequencies of 9, 12, 20, and 45.7 MHz by means of pulsed spectrometers already reported.^{9,12)} The conventional inversion recovery method was employed to determine T_1 values. DTA experiments were performed using a homemade apparatus.¹³⁾ For the foregoing measurements, temperatures were determined by use of copper constantan thermocouples with the accuracy of ± 3 K for the wide-line NMR and ± 1 K for the other measurements. X-Ray powder patterns were recorded at room temperature using a Model D-3F diffractometer from Rigaku Denki Co. equipped with a copper anticathode.

(tetMA)₂CdCl₄ was synthesized by slowly evaporating the solvent after mixing two methanol solutions of $2\text{CdCl}_2 \cdot \text{H}_2\text{O}$ and (tetMA)Cl in a molar ratio of 1:8.¹⁴⁾ (tetMA)₂CdBr₄ was prepared in a similar manner from the corresponding bromides. Crystals of these salts obtained were purified by recrystallization from methanol by adding a small amount of the corresponding tetramethylammonium halides. (tetMA)₂CdI₄ was obtained by mixing the aqueous solutions of stoichiometric amounts of CdI_2 and (tetMA)I. The colorless crystals obtained were recrystallized from water. The above crystals prepared and purified were dried over phosphorus pentoxide in a vacuum desiccator and were sealed in glass ampoules for the measurements of NMR and DTA after evacuating ambient air and then putting in a small amount of helium exchange gas. (tetMA)₂CdCl₄ and (tetMA)₂CdBr₄ were identified by chemical analysis. Anal. Calcd for $[(\text{CH}_3)_4\text{N}]_2\text{CdCl}_4$: Cl, 35.2; C, 23.9; H, 6.0%. Found: Cl, 35.1; C, 23.7; H, 6.1%. Calcd for $[(\text{CH}_3)_4\text{N}]_2\text{CdBr}_4$: Br, 55.1; C, 16.6; H, 4.2%. Found: Br, 55.0; C, 16.7; H, 4.2%. (tetMA)₂CdI₄ was identified by taking X-ray powder patterns. All diffrac-

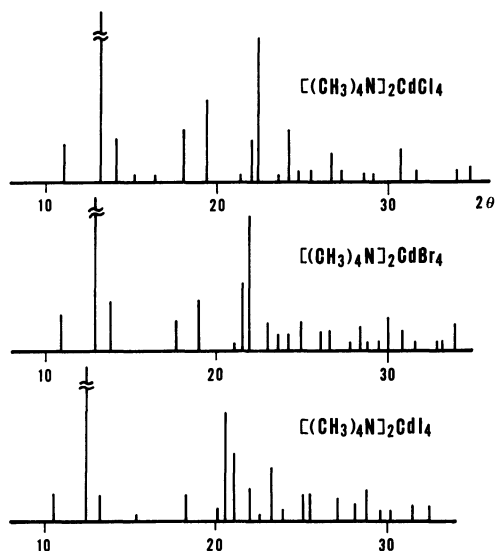


Fig. 1. X-Ray powder patterns taken at room temperature for tetramethylammonium tetrachloro- and tetrabromocadmata(II). Those of tetraiodocadmata(II) are given for comparison.

tion lines detected were completely indexed in terms of an orthorhombic lattice having the lattice constants $a=13.409$, $b=9.724$, and $c=16.894$ Å already reported by Kallel et al.¹⁵⁾

Results

From X-ray powder patterns taken at room temperature, the crystals of $(\text{tetMA})_2\text{CdCl}_4$ and $(\text{tetMA})_2\text{CdBr}_4$ were proved to be isomorphous with that of $(\text{tetMA})_2\text{CdI}_4$. The powder patterns recorded for the three complexes are shown in Fig. 1. These patterns could be interpreted by the orthorhombic structure of many $(\text{tetMA})_2\text{MX}_4$ type tetrahedral complexes¹⁶⁻¹⁸⁾ belonging to the space group $Pnma$ with $Z=4$. The lattice constants determined were $a=12.47$, $b=9.12$, and $c=15.81$ Å for $(\text{tetMA})_2\text{CdCl}_4$ and $a=12.78$, $b=9.33$, and $c=16.19$ Å for $(\text{tetMA})_2\text{CdBr}_4$.

DTA curves recorded between ca. 80 and 450 K for the three complexes are shown in Fig. 2.

When $(\text{tetMA})_2\text{CdCl}_4$ was heated from room temperature, a very small endothermic anomaly having a tail on the low temperature side appeared. The peak temperature of the anomaly was 399 K. An exothermic anomaly having a similar shape to the endothermic one and almost the same peak temperature appeared on cooling. Various methylammonium salts are known to show characteristic small heat anomalies showing no hysteresis phenomena about the peak temperature similar to the present one.^{13,19-23)} For these salts, we could unequivocally determine the phase transition temperature (T_{tr}) to be the peak temperature of DTA curves by comparing with the results of NQR studies which yield more accurate information about the alteration of crystal structure taking place especially in ionic crystals.^{13,19-24)} Accordingly, we can conclude

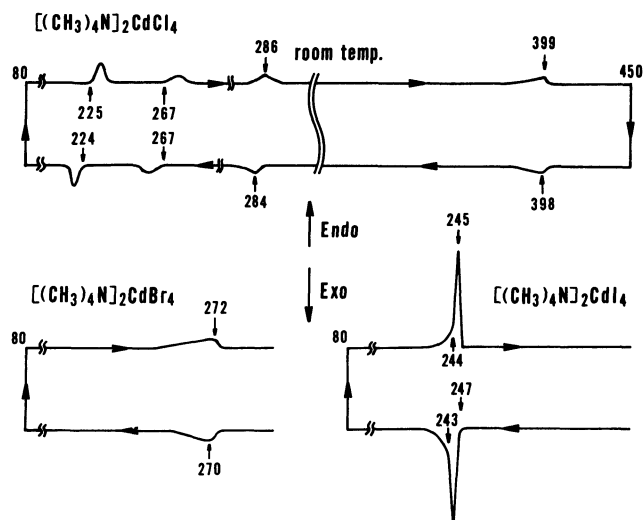


Fig. 2. DTA curves recorded for tetramethylammonium tetrachloro-, tetrabromo-, and tetraiodocadmata(II). Heat anomalies observed for tetrachlorocadmata(II) near 285 K are so small that they are enlarged about three times and shown in the figure. Temperatures measured in K are given only by figures.

that $(\text{tetMA})_2\text{CdCl}_4$ undergoes a second order phase transition at 399 K.

When $(\text{tetMA})_2\text{CdCl}_4$ was cooled from room temperature, three small exothermic anomalies appeared, the starting temperatures of which were 287, 267, and 224 K. Among these anomalies, the highest temperature one was very small. With increasing temperature, endothermic anomalies appeared at 225 and 267 K which were the initial temperatures and at 286 K determined as the peak temperature. Since the initiating temperature of the last one could hardly be determined because of its weakness and also broadness, we tentatively assigned T_{tr} of this phase transition as 286 K. Therefore, it is concluded that $(\text{tetMA})_2\text{CdCl}_4$ undergoes three phase transitions at 286, 267, and 225 K below room temperature. Consequently, this complex experiences totally four phase transitions between ca. 80 and 450 K, yielding five structurally different solid phases.

Below room temperature, when $(\text{tetMA})_2\text{CdBr}_4$ was cooled and warmed, an exothermic and an endothermic anomaly, respectively, appeared. Both anomalies are small and bear a strong resemblance to those observed at T_{tr} of 399 K for $(\text{tetMA})_2\text{CdCl}_4$. They gave almost the same peak temperature. Except these, no heat anomaly could be recorded on both cooling and heating runs between ca. 80 and 430 K. Accordingly, one can conclude that $(\text{tetMA})_2\text{CdBr}_4$ exhibits only one phase transition at 272 K, indicating the presence of two different crystalline phases.

With decreasing the temperature from room temperature, $(\text{tetMA})_2\text{CdI}_4$ yielded a large exothermic peak which started very sharply at 247 K. From the peak

temperature, the curve returned back very sharply and almost symmetrically, but it became asymmetric from 243 K and gradually returned back to the base line with decreasing temperature. When the temperature was increased from 80 K, the base line was gradually deviated to the endothermic direction from ca. 235 K and a very sharp and large peak started from 244 K. The curve reached the maximum at 245 K, above which temperature the curve returned back to the base line very sharply. These experimental facts suggest that there exist two successive phase transitions around 245 K in the crystal of $(\text{tetMA})_2\text{CdI}_4$. Since these phase transitions were not resolved, we could not determine T_{tr} exactly. Therefore, $(\text{tetMA})_2\text{CdI}_4$ can be considered to undergo successive phase transitions having considerably different nature around 245 K. No heat anomaly except the above ones was recorded between ca. 80 and 450 K.

The temperature dependence of ^1H T_1 observed for $(\text{tetMA})_2\text{CdCl}_4$ at the Larmor frequency of 20 MHz in a temperature range of 85–430 K is shown in Fig. 3. Two clearly separable T_1 minima with almost the same minimum value of 16 ms were observed. It is quite interesting that the observed T_1 curve is smooth and shows no marked anomaly at the phase transitions revealed by the DTA experiments although the gradient of the T_1 curve becomes milder just above T_{tr} of 286 K. This indicates that the phase transitions at 399, 267, and 225 K give negligible influence on the averaging of ^1H – ^1H dipolar interac-

tions in the cation.

The temperature dependences of ^1H T_1 observed for $(\text{tetMA})_2\text{CdBr}_4$ at 12 and 20 MHz in the temperature ranges 300–465 K and 56–430 K, respectively, are

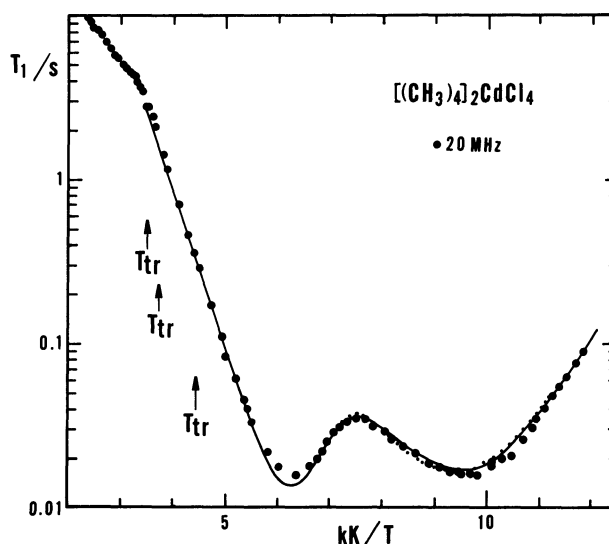


Fig. 3. Temperature dependence of ^1H T_1 observed for tetramethylammonium tetrachlorocadmate(II) at the Larmor frequency of 20 MHz (●). Solid line indicates the best fitted T_1 curve calculated based on the cationic model of C_{3v} while dotted line that based on the model of C_{2v} . Both curves agree very well with experimental values. The dotted line is written only in the temperature region where both calculated curves differ from one another. T_{tr} is the phase transition temperature determined by DTA.

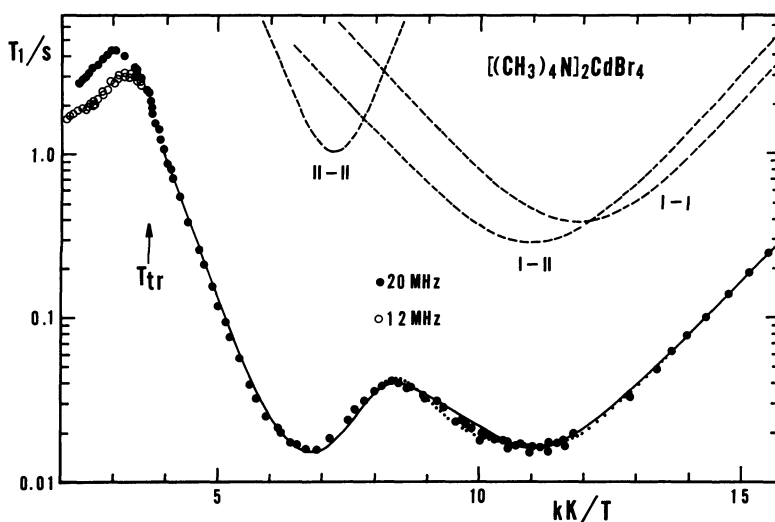


Fig. 4. Temperature dependence of ^1H T_1 observed for tetramethylammonium tetrabromocadmate(II) at the resonance frequencies of 20 (●) and 12 (○) MHz. Solid line shows the best fitted T_1 curve calculated using the cationic model of C_{3v} while dotted line that using the model of C_{2v} . The dotted curve is written only in the temperature region where both calculated curves differ from one another. Broken lines show calculated T_1 curves arising from inter-cationic dipolar interactions. Three curves were calculated for the cations between the same kind I(I-I), the different kinds I and II(I-II), and the same kind II(II-II). T_{tr} denotes the phase transition temperature determined from DTA.

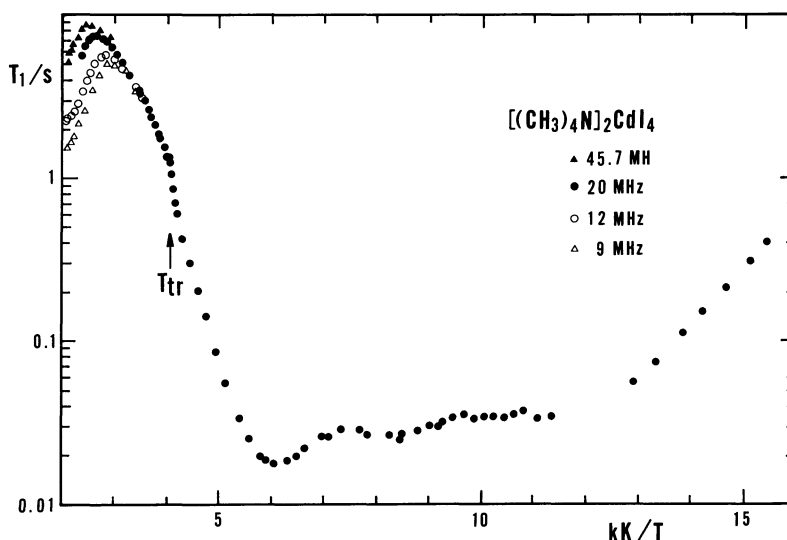


Fig. 5. Temperature dependence of ^1H T_1 , observed for tetramethylammonium tetraiodocadmate(II) at 45.7 (\blacktriangle), 20 (\bullet), 12 (\circ), and 9 (Δ) MHz. T_{tr} indicates the phase transition temperature determined by DTA.

shown in Fig. 4. Two T_1 minima having almost the same minimum value of 16 ms were also obtained for this complex below T_{tr} . The T_1 curve yielding the low temperature minimum was very broad. The same is true for $(\text{tetMA})_2\text{CdCl}_4$. Above T_{tr} , ^1H T_1 curves observed at both frequencies showed a maximum, above which temperature both T_1 values decreased almost linearly.

The temperature dependences of ^1H T_1 of $(\text{tetMA})_2\text{CdI}_4$ measured at 9, 12, 20, and 45.7 MHz are shown in Fig. 5. T_1 observation was made in the temperature ranges of 65–430 K for 20 MHz and 300–465 K for the other three frequencies. Possibly, three or four T_1 minima partially overlapped to each other could be seen below T_{tr} . In a narrow temperature range below T_{tr} of ca. 245 K, ^1H T_1 observed at 20 MHz increased rapidly with increasing temperature and gave, above T_{tr} , a milder temperature gradient. With further increasing temperature, ^1H T_1 observed at the above Larmor frequencies yielded a maximum above which temperature each T_1 decreased almost linearly.

Discussion

It has been reported,^{16–18)} that half of the eight cations in a unit cell ($Z=4$) of the isomorphous $(\text{tetMA})_2\text{MX}_4$ type complexes including $(\text{tetMA})_2\text{CdI}_4$ occupies one of two kinds of nonequivalent lattice sites having low site symmetry. This means that the cation in these crystals may be distorted to some extent mainly through the electrostatic forces of the neighboring ions. In fact, the cations in the crystals of $(\text{tetMA})_2\text{CdI}_4$ are known to be slightly distorted from T_d although the heavy atoms of the cation have very large thermal parameters.¹⁵⁾ In the following discussion, the same structures were roughly assumed for the cations also in $(\text{tetMA})_2\text{CdCl}_4$ and

$(\text{tetMA})_2\text{CdBr}_4$ crystals because no atomic coordinates have been determined for these complexes as yet.

The present DTA experiments revealed the existence of phase transitions for both chloride and bromide complexes below room temperature. This means that the crystal structure of these complexes at lower temperatures is no more the same as that determined at room temperature. However, the heat anomalies recorded were so small that the structure was expected to be altered only slightly by the phase transitions. Furthermore, the ^1H T_1 data obtained show no marked anomaly at T_{tr} suggesting that the cations in these crystals keep almost the same structure from room temperature down to below 77 K.

According to the BPP theory, ^1H T_1 arising from the averaging of ^1H – ^1H magnetic dipolar interactions due to molecular motions can be expressed as²⁵⁾

$$T_1^{-1} = Cg(\tau), \quad (1)$$

where

$$g(\tau) = \tau/(1 + \omega^2\tau^2) + 4\tau/(1 + 4\omega^2\tau^2). \quad (2)$$

In these equations, C , τ , and ω denote the motional constant, the correlation time of the motion, and the angular Larmor frequency, respectively. By assuming the Arrhenius relationship for the motion, τ can be written using the activation energy E_a for the motion as

$$\tau = \tau_0 \exp(E_a/RT), \quad (3)$$

where τ_0 is the correlation time at the limit of infinite temperature.

The fact that the two T_1 minima with the same minimum value were observed for both chloride and

bromide complexes agrees very well with the crystal structure described above, showing the existence of two nonequivalent $(\text{tetMA})^+$ cations in the crystal. Conceivable motional modes of the cation contributing to the T_1 minima are reorientations of the four CH_3 groups in the cation and also of the slightly distorted cation as a whole about its real and/or fictitious C_2 and C_3 symmetry axes. A possible explanation of the fairly deep T_1 minimum of 16 ms determined for each of the two nonequivalent cations is that all of these motional modes of each cation give a T_1 minimum at almost the same temperature and contribute as a whole to the T_1 minimum. This is because the ^1H T_1 minimum of the cation arising from these motional modes can be roughly estimated as 14 ms,⁹⁾ although this is obtained by assuming that all bond angles in the cation are tetrahedral and the bond lengths of C-H and C-N are 1.09 and 1.50 Å, respectively.¹⁾

$(\text{tetMA})_2\text{CdCl}_4$ and $(\text{tetMA})_2\text{CdBr}_4$ yielded very gentle gradients of $\log T_1$ vs. T^{-1} plots on the cold side of the lower temperature T_1 minimum. By using Eqs. 1–3, we roughly estimated E_a as 9 and 6.5 kJ mol⁻¹ for the chloride and bromide complexes, respectively, from each slope. These values are too small to be considered mostly resulting from the CH_3 C_3 reorientation by the following reasons. The potential barriers for the internal CH_3 rotation in the cation have been estimated as 19.3 and 17.6 kJ mol⁻¹ for $(\text{tetMA})_2\text{PtCl}_6$ and $(\text{tetMA})_2\text{PtBr}_6$, respectively, from the study of vibrational spectra.^{26,27)} For molecules having CH_3 groups in a similar situation to that of the cation, the torsional barriers of CH_3 groups in $(\text{CH}_3)_3\text{N}$ and $(\text{CH}_3)_4\text{C}$ molecules are reported to be 18.5 and 18.0 kJ mol⁻¹, respectively.^{28,29)} Moreover we also already obtained E_a for the CH_3 C_3 reorientation of the cation in $(\text{tetMA})_2\text{MBr}_6$ (M=Sn, Te, Pt) crystals as 15.4, 17.8, and 18.4 kJ mol⁻¹ respectively.¹⁰⁾

In previous papers,^{9,10)} we explained shallow T_1 minima with extremely low E_a values (≈ 8 kJ mol⁻¹) appearing at lower temperatures for $(\text{tetMA})_2\text{TeCl}_6$, $(\text{tetMA})_2\text{PtCl}_6$, and $(\text{tetMA})_2\text{MBr}_6$ (M=Sn, Te, Pt) by the small-angle reorientation of the four CH_3 groups about their respective C_3 axis. However, this process can be permitted only for the cation placed in a highly symmetrical and weak crystal field such as that in the above complexes. This is because the correlated reorientation of the four CH_3 groups is an important condition for this motion. Since the cations in the present complexes are located at low symmetric lattice sites, their structure must be deformed from a tetrahedron. Therefore, the small-angle reorientation seems to be unsuitable for the explanation of the present T_1 minima with small E_a appearing at lower temperatures. For the cations deformed to some extent such as those in the present complexes, it can be expected that E_a for one or two CH_3 groups in the cation may be much lower than that for the others. This is because hindering barrier for the CH_3 C_3 reorientation

is considered to be formed mainly by the intraionic forces.

For the present complexes, the CH_3 C_3 and overall reorientations give T_1 minima at almost the same temperature, where the condition necessary for the conventional treatment by Albert et al.⁹⁾ is not fulfilled. This indicates that this usual method cannot be used here. To interpret the present T_1 data, we employed the method of T_1 calculation reported by Takeda et al.,³⁰⁾ which had been used for the interpretation of the data observed for neopentane. In this method, pairwise addition of intra- and inter-methyl ^1H magnetic dipolar interactions is taken for randomly jumping ^1H – ^1H vectors through the respective CH_3 C_3 reorientations and also the reorientations of the whole cation about its C_2 and C_3 axes. Since jumping of each ^1H – ^1H vector is regarded as representable by a Markov process, no correlation between these motions is considered as like in the case of the more convenient and widely used method developed by Albert et al.⁹⁾

In the following analysis of T_1 , the presence of two kinds of nonequivalent $(\text{tetMA})^+$ cations is assumed in accordance with the crystal structure isomorphous with $(\text{tetMA})_2\text{CdI}_4$ and the other $(\text{tetMA})_2\text{MX}_4$ type complexes.^{15–18)} In the structure, each cation is placed on a mirror plane of the unit cell, indicating that there exist two equivalent carbon atoms in the cation. This means that each cation has two or three nonequivalent CH_3 groups. For favorable cases, the cations having C_{2v} or C_{3v} symmetry can be placed on the lattice sites. Therefore, the present T_1 calculation was performed for the two models of the cations having C_{2v} or C_{3v} symmetry so far as the motion of CH_3 groups is concerned. In other words, the geometry of the cation was roughly assumed to be T_d but the motional states of the four CH_3 groups to satisfy the above symmetry. The stable positions of hydrogen atoms were fixed at the all-staggered conformation,²⁷⁾ and for C-H and C-N bond lengths the foregoing values were used.⁹⁾

As the first model, we consider the cation having C_{2v} symmetry only in the motional states of the four CH_3 groups. Namely, two pairs, each of which consists of "equivalent" CH_3 groups, have different jumping rates and activation energies for the CH_3 C_3 reorientations from one another. For overall cationic reorientations, we assumed the presence of two kinds of nonequivalent C_2 reorientations about one genuine C_2 and two pseudo C_2 axes of the cation and, for simplicity, a single kind of C_3 reorientation about the four pseudo C_3 axes.

As the second model, we assumed the cation having C_{3v} symmetry in the same sense as above. In this model, we assumed that one CH_3 group of the cation has a more frequent jumping rate and a lower activation energy for the C_3 reorientation than the other three groups. The whole cationic motions are considered to consist of C_3 reorientations about the unique C_3 axis and the other three pseudo C_3 axes, and of C_2

reorientations about the three equivalent pseudo C_2 axes of the cation. In general, these reorientational modes should have different correlation times with the temperature dependence expressed by Eq. 3. However, the overall cationic C_3 and C_2 reorientations were reasonably assumed to have the same τ_0 and the same assumption could be made on the two kinds of CH_3 C_3 reorientations as well.

For the first C_{2v} model, the 12×12 transition matrix $D^{30)}$ to calculate the intra CH_3 relaxation rate due to random jumpings of the ^1H - ^1H vectors is given by

$$D = \begin{pmatrix} A & B & B' & B' \\ B & A & B' & B' \\ B' & B' & A' & B \\ B' & B' & B & A' \end{pmatrix}, \quad (4)$$

where

$$A = \begin{pmatrix} a_0 & a_1 & a_1 \\ a_1 & a_0 & a_1 \\ a_1 & a_1 & a_0 \end{pmatrix}, \quad A' = \begin{pmatrix} a_0' & a_1' & a_1' \\ a_1' & a_0' & a_1' \\ a_1' & a_1' & a_0' \end{pmatrix}, \quad (5)$$

$$B = -\begin{pmatrix} \omega_2 & \omega_3' & \omega_3' \\ \omega_3' & \omega_2 & \omega_3' \\ \omega_3' & \omega_3' & \omega_2 \end{pmatrix}, \quad B' = -\begin{pmatrix} \omega_2' & \omega_3' & \omega_3' \\ \omega_3' & \omega_2' & \omega_3' \\ \omega_3' & \omega_3' & \omega_2' \end{pmatrix}. \quad (5')$$

In these equations,

$$a_0 = 2\omega_{\text{CH}_3} + 8\omega_3' + \omega_2 + 2\omega_2', \quad (6)$$

$$a_1 = -(\omega_{\text{CH}_3} + \omega_3'), \quad (7)$$

$$a_0' = 2\omega_{\text{CH}_3}^* + 8\omega_3' + \omega_2 + 2\omega_2', \quad (8)$$

$$a_1' = -(\omega_{\text{CH}_3}^* + \omega_3'). \quad (9)$$

Here, ω_{CH_3} and $\omega_{\text{CH}_3}^*$ are the jumping rates of the C_3 reorientations of two nonequivalent CH_3 groups, and ω_2 , ω_2' , and ω_3' denote the jumping rates of the whole cationic reorientations about the C_2 , pseudo C_2 , and pseudo C_3 axes, respectively. These jumping rates were assumed to be the reciprocals of the correlation times of these motions.

The transition matrix due to jumping of the inter CH_3 ^1H - ^1H vectors was calculated in a similar manner as used by Takeda et al.³⁰⁾ Since diagonalization of these transition matrices which could be algebraically done for the T_d symmetric molecule was difficult for the present systems, it was carried out numerically using a FACOM-M382 computer in the Computation Center of Nagoya University.

Correlation times for the respective motional modes at a fixed temperature were calculated using Eq. 3 by substituting suitable trial values of E_a and τ_0 . The numerical D matrix can be expressed in terms of these correlation times. By diagonalizing the D matrix thus constructed, we obtained a set of non-trivial

eigenvalues which were reciprocals of the correlation times for the normal modes of reorientations for the intra CH_3 ^1H - ^1H vectors at the temperature. The calculation for the D matrix of the jumping of the inter ^1H - ^1H vectors was performed analogously. Finally, ^1H T_1 was obtained by the following equation,

$$T_1^{-1} = \sum_{\ell} K_{\ell} \left(\frac{\tau_{\ell}}{1 + \omega^2 \tau_{\ell}^2} + \frac{4\tau_{\ell}}{1 + 4\omega^2 \tau_{\ell}^2} \right), \quad (10)$$

where τ_{ℓ} and K_{ℓ} indicate the correlation time of the ℓ -th normal mode associated with intra and inter ^1H - ^1H vector jumpings and a constant depending on the mode and the structure as well, respectively. K_{ℓ} can be calculated numerically using the equations given by Takeda et al.³⁰⁾

T_1 values in a wide range of temperature were calculated as above by changing seven unknown parameters i.e., five E_a and two τ_0 values. From the T_1 curves calculated here, we selected several curves which agreed roughly with the observed values obtained from the cold side of the T_1 minimum, and derived approximate values of the unknown parameters.

For the other T_1 curve appearing at higher temperatures, the same method of calculation was applied. However, the T_1 curve having a rather steep slope may be interpreted by the usual "undistorted" cation. Therefore, the calculation was performed by simply assuming that all CH_3 groups in the cation are equivalent even in their motion. This results in the reduction of the number of unknown parameters.

The theoretical T_1 curve for the second model of the cation with C_{3v} symmetry for the motion of the CH_3 groups could be obtained similarly using the D matrix given by

$$D = \begin{pmatrix} A' & B_1 & B_2 & B \\ B_2 & A' & B_1 & B \\ B_1 & B_2 & A' & B \\ B & B & B & A \end{pmatrix}, \quad (11)$$

where

$$A = \begin{pmatrix} a_0 & a_1 & a_1 \\ a_1 & a_0 & a_1 \\ a_1 & a_1 & a_0 \end{pmatrix}, \quad A' = \begin{pmatrix} a_0' & a_1' & a_1' \\ a_1' & a_0' & a_1' \\ a_1' & a_1' & a_0' \end{pmatrix}, \quad (12)$$

$$B_1 = -\begin{pmatrix} \omega_2' & \omega_3' & \omega_3' \\ \omega_3' & \omega_2' & \omega_3' \\ \omega_3' & \omega_3' & \omega_2' \end{pmatrix}, \quad B_2 = -\begin{pmatrix} \omega_2' & \omega_3 & \omega_3' \\ \omega_3' & \omega_2' & \omega_3 \\ \omega_3 & \omega_3' & \omega_2' \end{pmatrix},$$

$$B = -\begin{pmatrix} \omega_2' & \omega_3' & \omega_3' \\ \omega_3' & \omega_2' & \omega_3' \\ \omega_3' & \omega_3' & \omega_2' \end{pmatrix}. \quad (13)$$

In these matrices,

$$a_0 = 2\omega_{\text{CH}_3} + 2\omega_3 + 6\omega_3' + 3\omega_2', \quad (14)$$

$$a_1 = -(\omega_{\text{CH}_3} + \omega_3), \quad (15)$$

$$a_0' = 2\omega_{\text{CH}_3}^* + 2\omega_3 + 6\omega_3' + 3\omega_2', \quad (16)$$

$$a_1' = -(\omega_{\text{CH}_3}^* + \omega_3'). \quad (17)$$

Here, ω_{CH_3} and ω_3 are the jumping rates of the ^1H - ^1H vectors for the CH_3 C_3 and the whole cationic C_3 reorientations about the unique C_3 axis of the cation, respectively. $\omega_{\text{CH}_3}^*$ is the jumping rate of the other CH_3 C_3 reorientation while ω_3' and ω_2' denote those of the whole cationic reorientations about the other three pseudo C_3 and the three pseudo C_2 axes, respectively.

Since these ^1H - ^1H vector reorientations in the cations should also average the interionic dipolar interactions which might be small, the interionic contribution to T_1 was roughly estimated by evaluating the difference of the inter-cationic second moment ΔM_2 between those in the rigid lattice and in the isotropically rotating state. The second moment M_2 in the rigid lattice could be roughly estimated for the present complexes by placing the T_d cations in the crystalline lattice isomorphous with $(\text{tetMA})_2\text{CdI}_4$. From this model, we could calculate inter-protonic distances between protons belonging to the different cations. The interionic M_2 averaged by rapid ionic rotations was obtained by use of the method reported by Andrew and Eades.³¹⁾ In both crystals, there are two kinds of the cations I and II, which are considered to perform isotropic rotation with quite different correlation times from each other. Then, T_1 for the cation I giving rise to the low temperature minimum is expressed by^{32,33)}

$$T_1^{-1} = \frac{2}{3}\gamma^2\Delta M_2g(\tau_{\text{iso}}) + \frac{2}{3}\gamma^2\Delta M_2'g(\tau_{\text{iso}}/2), \quad (18)$$

where γ and τ_{iso} indicate the gyromagnetic ratio of a proton and the correlation time of the isotropic rotation of the cation I, respectively.

The first term of Eq. 18 comes from the ^1H dipolar interactions between the cations I and II, while the second arises from those between protons belonging to the same kind of the cations I. The values of ΔM_2 and $\Delta M_2'$ calculated were 0.64 and 0.48 G^2 , respectively. To evaluate τ_{iso} which is assumed to be expressed by Eq. 3, let the T_1 minimum temperature for the first term of Eq. 18 be equal to that of the observed low temperature one. Then, the temperature dependence of τ_{iso} was roughly estimated from the slope of the $\log T_1$ vs. T^{-1} curve. For the cation II yielding the high temperature T_1 minimum, the interionic T_1 can be given only by the second term of Eq. 18. $\Delta M_2'$ for this cation was calculated as 0.18 G^2 and τ_{iso} was obtained in the same way as for the cation I. The interionic contribution to the calculation of ^1H T_1 was taken into account only for $(\text{tetMA})_2\text{CdBr}_4$ because it was turned out to be very small and the observed ^1H T_1 for $(\text{tetMA})_2\text{CdCl}_4$ was assumed to be well explained only by intraionic contribution.

The refinement of the foregoing calculation was finally performed by changing the values of the adjustable parameters by stepwise finely to obtain the resultant best fitted T_1 curve which was the sum of the low and high temperature T_1 curves calculated separately as above. The evaluation of the degree of fitting was determined by inspection.

The most appropriate T_1 curves calculated for the two kinds of the models of the cation are shown in Figs. 3 and 4 for the chloride and bromide complexes, respectively. The adjustable parameters giving rise to these T_1 curves are shown in Table 1. From these results, it is difficult to determine which model is more suitable for the present complexes. This is because both models provided the T_1 curves interpreting the observed T_1 data very well. However, it can be said that the observed T_1 curve having a normal minimum value but unusually small E_a can be explained by the motionally distorted T_d cation.

The values of E_a derived from the low temperature T_1 curve indicate that there is a distinct difference between the reorientations of the two kinds of CH_3 groups in the cation. It is noteworthy that E_a for the CH_3 reorientation whose rate is given by $\omega_{\text{CH}_3}^*$ is rather insensitive to the shape of the T_1 curve for both complexes and also for the choice of the model of the cation when E_a is larger than ca. 12 kJ mol^{-1} . On the other hand, the other E_a values listed in Table 1 gave an appreciable change on the shape of the curve when they were altered more than 0.5 kJ mol^{-1} . The larger E_a values of $(\text{tetMA})_2\text{CdCl}_4$ than those of $(\text{tetMA})_2\text{CdBr}_4$ obtained from both models are understandable by considering the size effect of the anion. Namely, the cations in the latter complex are thought to be more loosely packed in the crystal than those in the former crystal.

The T_1 curve observed for $(\text{tetMA})_2\text{CdI}_4$ below room temperature is quite different from those of the foregoing two complexes, although the three complexes are isomorphous at room temperature. This difference may be due to the phase transition located at ca. 245 K, which exhibits a large heat anomaly suggesting a drastic change of the crystal structure. Therefore, the appearance of many T_1 minima successively in the low temperature phase is possibly attributed to the existence of more than two nonequivalent cations and/or CH_3 groups in the cation yielding their T_1 minima due to reorientations appearing in a fairly wide range of temperature. For this complex, E_a values were roughly estimated from the linear portions on the hot and cold sides of the T_1 curve below T_{tr} as 20.7 and 6.5 kJ mol^{-1} , respectively. Very small E_a of 6.5 kJ mol^{-1} was obtained also for this complex in the very low temperature region.

A T_1 decrease with increasing temperature was observed for both $(\text{tetMA})_2\text{CdBr}_4$ and $(\text{tetMA})_2\text{CdI}_4$ above room temperature, indicating the presence of at least one new relaxation process at higher temperatures.

Table 1. Best Fitted Activation Energies E_a and Correlation Times τ_0 for ^1H - ^1H Vector Jumping Rates of the Cation in Tetramethylammonium (tetMA) Tetrachloro- and Tetrabromocadmate(II) Yielding High and Low Temperature T_1 Curves

| Compound [Motional model] | High temp side | | | Low temp side | | |
|---|--|--------------------------|-----------------------|--------------------------|--------------------------|-----------------------|
| | Jumping rate | $E_a/\text{kJ mol}^{-1}$ | τ_0/s | Jumping rate | $E_a/\text{kJ mol}^{-1}$ | τ_0/s |
| $(\text{tetMA})_2\text{CdCl}_4$ [C_{3v}] | ω_{CH_3} | 17.5 | 3.3×10^{-12} | ω_{CH_3} | 7.5 | 2.5×10^{-12} |
| | | | | $\omega_{\text{CH}_3}^*$ | >15.0 | |
| | ω_3 | 19.7 | 3.3×10^{-14} | ω_3 | 10.8 | 6.3×10^{-14} |
| | | 19.7 | | ω_3' | 18.0 | |
| | ω_2 | 18.1 | | ω_2' | 13.0 | |
| | [C_{2v}] ω_{CH_3} | 17.5 | 3.3×10^{-12} | ω_{CH_3} | 8.1 | 1.7×10^{-12} |
| | | | | $\omega_{\text{CH}_3}^*$ | >12.0 | |
| | | ω_3 | 3.2×10^{-14} | ω_2 | 11.0 | 3.3×10^{-14} |
| | | 19.7 | | ω_2' | 13.0 | |
| | | 18.0 | | ω_3' | 14.5 | |
| $(\text{tetMA})_2\text{CdBr}_4$ [C_{3v}] | ω_{CH_3} | 14.0 | 1.3×10^{-11} | ω_{CH_3} | 5.1 | 1.1×10^{-11} |
| | | | | $\omega_{\text{CH}_3}^*$ | >12.0 | |
| | ω_3 | 17.5 | 1.3×10^{-13} | ω_3 | 9.8 | 3.3×10^{-14} |
| | | 17.5 | | ω_3' | 12.7 | |
| | ω_2 | 14.5 | | ω_2' | 15.0 | |
| | [C_{2v}] ω_{CH_3} | 14.0 | 1.3×10^{-11} | ω_{CH_3} | 5.7 | 8.3×10^{-12} |
| | | | | $\omega_{\text{CH}_3}^*$ | >12.0 | |
| | | ω_3 | 1.3×10^{-11} | ω_2 | 9.5 | 3.3×10^{-12} |
| | | 17.5 | | ω_2' | 12.5 | |
| | | 14.5 | | ω_3' | 12.5 | |

In these temperature regions, a clear frequency dependence of ^1H T_1 was observed for both complexes. However, the ratios of T_1 values determined at different frequencies and at the same temperature are much smaller than those of squared resonance frequencies. We determined M_2 for $(\text{tetMA})_2\text{CdBr}_4$ at 450 K and yielded 0.5 G^2 which was almost the same as the value of 0.6 G^2 obtained at 302 K. This indicates that the T_1 decrease observed is difficult to explain through the magnetic dipolar relaxation mechanism.

It has been reported^{34,35} that even bulky octahedral complex anions such as $[\text{PtCl}_6]^{2-}$ and $[\text{PtBr}_6]^{2-}$ reorient quite frequently at high temperatures and this motion appreciably shortens spin-lattice and also spin-spin relaxation times of the quadrupolar halogen nuclei. In the present complexes, rapid motions of the complex anions can be also expected to take place at high temperatures and the quadrupole resonance frequencies of iodine and bromine in both complexes are nearer to the NMR frequencies than that of chlorine in $(\text{tetMA})_2\text{CdCl}_4$. Quadrupolar relaxation of iodine and bromine nuclei can provide an important relaxation process for ^1H in the cation through magnetic interactions between ^1H and halogen nuclei when the quadrupolar relaxation time becomes shorter than ^1H T_1 at high temperatures. This relaxation mechanism named dipolar relaxation of the second kind³⁶ seems to be the main origin of the frequency dependent T_1 decrease observed at higher temperatures.

This work was partially supported by a Grant-in-Aid

for Scientific Research No. 59470009 from the Ministry of Education, Science and Culture.

References

- 1) E. R. Andrew and P. C. Canepa, *J. Magn. Reson.*, **7**, 429 (1972).
- 2) M. Mahajan and B. D. Nageswara Rao, *J. Phys. C*, **7**, 995 (1974).
- 3) S. Albert, H. S. Gutowsky, and J. A. Ripmeester, *J. Chem. Phys.*, **56**, 3672 (1972).
- 4) A. A. V. Gibson and R. E. Raab, *J. Chem. Phys.*, **57**, 4688 (1972).
- 5) H. Rager and A. Weiss, *Z. Phys. Chem.*, **NF93**, 299 (1974).
- 6) T. Tsuneyoshi, N. Nakamura, and H. Chihara, *J. Magn. Reson.*, **27**, 191 (1977).
- 7) H. Rager and A. Weiss, *Ber. Bunsenges. Phys. Chem.*, **80**, 138 (1976).
- 8) H. Rager and A. Weiss, *Ber. Bunsenges. Phys. Chem.*, **82**, 535 (1978).
- 9) L. S. Prabhumirashi, R. Ikeda, and D. Nakamura, *Ber. Bunsenges. Phys. Chem.*, **85**, 1142 (1981).
- 10) S. Sato, R. Ikeda, and D. Nakamura, *Ber. Bunsenges. Phys. Chem.*, **86**, 936 (1982).
- 11) T. Tsang and D. B. Utton, *J. Chem. Phys.*, **64**, 3780 (1976).
- 12) S. Gima, Y. Furukawa, R. Ikeda, and D. Nakamura, *J. Mol. Struct.*, **111**, 189 (1983).
- 13) Y. Kume, R. Ikeda, and D. Nakamura, *J. Magn. Reson.*, **33**, 331 (1979).
- 14) J. J. Foster and N. S. Gill, *J. Chem. Soc. (A)*, **1968**, 2625.
- 15) A. Kallel, J. W. Bats, and A. Daoud, *Acta Crystallogr., Sect. B*, **37**, 676 (1981).

- 16) B. Kamenar and A. Nagl, *Acta Crystallogr., Sect. B*, **32**, 1414 (1976).
 - 17) J. R. Wiesner, R. C. Srivastava, C. H. L. Kennard, M. Divaiva, and E. C. Lingafelter, *Acta Crystallogr.*, **23**, 565 (1967).
 - 18) P. Trouelan, J. Lefebvre, and P. Derollez, *Acta Crystallogr., Sect. C*, **40**, 386 (1984).
 - 19) Y. Kume, R. Ikeda, and D. Nakamura, *J. Magn. Reson.*, **20**, 276 (1975).
 - 20) Y. Kume, R. Ikeda, and D. Nakamura, *J. Phys. Chem.*, **82**, 1926 (1978).
 - 21) H. Ishida, R. Ikeda, and D. Nakamura, *J. Phys. Chem.*, **86**, 1003 (1982).
 - 22) H. Ishida, R. Ikeda, and D. Nakamura, *Phys. Stat. Sol. (a)*, **70**, K151 (1982).
 - 23) H. Ishida, R. Ikeda, and D. Nakamura, *Bull. Chem. Soc. Jpn.*, **59**, 915 (1986).
 - 24) G. Jugie and J. A. S. Smith, *J. Chem. Soc., Faraday Trans. 2*, **74**, 994 (1978).
 - 25) N. Bloembergen, E. M. Purcell, and R. V. Pound, *Phys. Rev.*, **73**, 679 (1948).
 - 26) R. W. Berg, *J. Chem. Phys.*, **69**, 1325 (1978).
 - 27) R. W. Berg, *J. Chem. Phys.*, **71**, 2531 (1979).
 - 28) W. G. Fateley and F. A. Miller, *Spectrochim. Acta*, **18**, 977 (1962).
 - 29) J. R. Durig, S. M. Craven, and J. Bragin, *J. Chem. Phys.*, **52**, 2046 (1969).
 - 30) S. Takeda, G. Soda, and H. Chihara, *Mol. Phys.*, **47**, 501 (1982).
 - 31) E. R. Andrew and R. G. Eades, *Proc. Roy. Soc. A*, **216**, 398 (1953).
 - 32) G. Soda and H. Chihara, *J. Phys. Soc. Jpn.*, **36**, 954 (1974).
 - 33) J. E. Anderson, *J. Chem. Phys.*, **43**, 3575 (1965).
 - 34) K. R. Jeffrey and R. L. Armstrong, *Phys. Rev.*, **174**, 359 (1968).
 - 35) M. Wiszniewska and R. L. Armstrong, *Can. J. Phys.*, **51**, 781 (1973).
 - 36) M. O. Norris, J. H. Strange, J. G. Powles, M. Rhodes, K. Marsden, and K. Krynicki, *J. Phys. C*, **1**, 422 (1968).
-